

Multiethnic genome-wide meta-analysis of ectopic fat depots identifies loci associated with adipocyte development and differentiation

AUTHOR BLOCK

Audrey Y Chu^{1,2,48}, Xuan Deng^{3,48}, Virginia A Fisher^{3,48}, Alexander Drong⁴, Yang Zhang^{5,6}, Mary F Feitosa⁷, Ching-Ti Liu³, Olivia Weeks⁶, Audrey C Choh⁸, Qing Duan⁹, Thomas D Dyer¹⁰, John D Eicher¹, Xiuqing Guo¹¹, Nancy L Heard-Costa³, Tim Kacprowski^{12,13}, Jack W Kent Jr¹⁴, Leslie A Lange⁹, Xinggang Liu¹⁵, Kurt Lohman^{16,17}, Lingyi Lu¹⁷, Anubha Mahajan⁴, Jeffrey R O'Connell¹⁵, Ankita Parihar¹⁵, Juan M Peralta¹⁰, Albert V Smith^{18,19}, Yi Zhang²⁰, Georg Homuth¹², Ahmed H Kissebah^{20,49}, Joel Kullberg²¹, René Laqua²², Lenore J Launer²³, Matthias Nauck^{24,13}, Michael Olivier^{14,20}, Patricia A Peyser²⁵, James G Terry²⁶, Mary K Wojczynski⁷, Jie Yao¹¹, Lawrence F Bielak²⁵, John Blangero¹⁰, Ingrid B Borecki⁷, Donald W Bowden^{27,28}, John Jeffrey Carr²⁶, Stefan A Czerwinski²⁹, Jingzhong Ding^{16,30}, Nele Friedrich^{24,13}, Vilmunder Gudnason^{18,19}, Tamara B Harris²³, Erik Ingelsson^{31,32}, Andrew D Johnson¹, Sharon LR Kardia²⁵, Carl D Langefeld¹⁷, Lars Lind²¹, Yongmei Liu^{16,33}, Braxton D Mitchell^{15,34}, Andrew P Morris^{35,4}, Thomas H Mosley Jr³⁶, Jerome I Rotter¹¹, Alan R Shuldiner¹⁵, Bradford Towne⁸, Henry Völzke^{37,13,38}, Henri Wallaschofski²⁴, James G Wilson³⁹, Matthew Allison⁴⁰, Cecilia M Lindgren⁴¹, Wolfram Goessling^{6,42,43,44,45}, L Adrienne Cupples^{1,3,50}, Matthew L Steinhauser^{5,6,45,46,50}, Caroline S Fox^{1,47,50}

AFFILIATIONS

1. NHLBI's Framingham Heart Study, Framingham MA USA
2. Division of Preventive Medicine, Brigham and Women's Hospital and Harvard Medical School, Boston MA USA
3. Department of Biostatistics, Boston University School of Public Health, Boston MA USA
4. Wellcome Trust Centre for Human Genetics, University of Oxford, Oxford UK
5. Department of Medicine, Brigham and Women's Hospital and Harvard Medical School, Boston MA USA
6. Division of Genetics, Brigham and Women's Hospital and Harvard Medical School, Boston MA USA
7. Department of Genetics, Washington University, St. Louis MO USA
8. Division of Epidemiology and Biostatistics, Department of Population and Public Health Sciences, Wright State University Boonshoft School of Medicine, Dayton OH USA
9. Department of Genetics, University of North Carolina, Chapel Hill NC USA
10. South Texas Diabetes and Obesity Institute, University of Texas Health Science Center at San Antonio & University of Texas of the Rio Grande Valley, Brownsville TX USA
11. Institute for Translational Genomics and Population Sciences, Department of Pediatrics, LABioMed at Harbor-UCLA Medical Center, Torrance CA USA

- 41 12. Interfaculty Institute for Genetics and Functional Genomics, University Medicine
42 Greifswald, Greifswald Germany
- 43 13. German Centre for Cardiovascular Research (DZHK), Partner Site Greifswald, Germany
- 44 14. TOPS Nutrition and Obesity Research Center, Department of Genetics, Texas
45 Biomedical Research Institute, San Antonio TX USA
- 46 15. University of Maryland School of Medicine, Baltimore MD USA
- 47 16. Wake Forest School of Medicine, Winston-Salem NC USA
- 48 17. Department of Biostatistical Sciences, Wake Forest School of Medicine, Winston-Salem
49 NC USA
- 50 18. Icelandic Heart Association, Kopavogur Iceland
- 51 19. Faculty of Medicine, University of Iceland, Reykjavik Iceland
- 52 20. TOPS Obesity and Metabolic Research Center, Biotechnology and Bioengineering
53 Center, Department of Physiology at the Medical College of Wisconsin, WI USA
- 54 21. Department of Surgical Sciences, Section of Radiology, Uppsala University, Uppsala
55 Sweden
- 56 22. Department of Neuroradiology, University Hospital Berne, Berne Switzerland
- 57 23. National Institute on Aging, Intramural Research Program, National Institutes of Health,
58 Bethesda MD USA
- 59 24. Institute for Clinical Chemistry and Laboratory Medicine, University Medicine Greifswald,
60 Greifswald Germany
- 61 25. Department of Epidemiology, School of Public Health, University of Michigan, Ann Arbor
62 MI USA
- 63 26. Departments of Radiology and Radiologic Sciences, Cardiovascular Medicine and
64 Biomedical Informatics, Vanderbilt University Medical Center, Nashville TN USA
- 65 27. Center for Genomics and Personalized Medicine Research, Wake Forest University
66 Health Sciences, Winston-Salem NC USA
- 67 28. Department of Biochemistry, Center for Diabetes Research, and Center for Human
68 Genomics, Wake Forest University School of Medicine, Winston-Salem NC USA
- 69 29. Department of Epidemiology, Human Genetics and Environmental Sciences, University
70 of Texas Health Science Center (UTHealth) School of Public Health Brownsville
71 Campus, Brownsville TX USA
- 72 30. Gerontology and Geriatric Medicine, Wake Forest School of Medicine, Winston-Salem
73 NC USA
- 74 31. Department of Medical Sciences, Molecular Epidemiology and Science for Life
75 Laboratory, Uppsala University, Uppsala Sweden
- 76 32. Department of Medicine, Division of Cardiovascular Medicine, Stanford University
77 School of Medicine, Stanford CA USA
- 78 33. Department of Epidemiology and Prevention, Wake Forest School of Medicine, Winston-
79 Salem NC USA
- 80 34. Geriatrics Research and Education Clinical Center, Baltimore Veterans Administration
81 Medical Center, Baltimore MD USA
- 82 35. Department of Biostatistics, University of Liverpool, Liverpool UK
- 83 36. University of Mississippi Medical Center, Jackson MS USA
- 84 37. Institute for Community Medicine, University Medicine Greifswald, Greifswald Germany

38. German Centre for Diabetes Research (DZD), Site Greifswald, Germany
39. Department of Physiology and Biophysics, University of Mississippi Medical Center,
Jackson MS USA
40. Division of Preventive Medicine, Department of Family Medicine and Public Health, UC
San Diego School of Medicine, San Diego CA USA
41. Li Ka Shing Centre for Health Information and Discovery, The Big Data Institute,
University of Oxford, Oxford, UK.
42. Harvard Stem Cell Institute, Cambridge MA USA
43. Gastroenterology Division, Brigham and Women's Hospital, Harvard Medical School,
Boston MA USA
44. Dana-Farber Cancer Institute, Boston MA USA
45. Broad Institute of MIT and Harvard, Cambridge MA USA
46. Division of Cardiovascular Medicine, Brigham and Women's Hospital and Harvard
Medical School, Boston MA USA
47. Division of Endocrinology, Brigham and Women's Hospital and Harvard Medical School,
Boston MA USA
48. These authors contributed equally to this work
49. This author is deceased
50. These authors jointly supervised this work

Correspondence should be addressed to AYC (audrey.chu@nih.gov), MLS
(msteinhauser@partners.org), or CSF (foxca@nhlbi.nih.gov)

ADDRESSES FOR CORRESPONDENCE:

Audrey Y Chu, PHD
NHLBI's Framingham Heart Study
Framingham MA 01702 USA
audrey.chu@nih.gov

Matthew L. Steinhauser, MD
Brigham and Women's Hospital and Harvard Medical School
Boston MA 02115 USA
msteinhauser@partners.org

Caroline S Fox, MD MPH
NHLBI's Framingham Heart Study
Framingham MA 01702 USA
foxca@nhlbi.nih.gov

KEY WORDS: GWAS, obesity, ectopic fat, adipocyte development, differentiation

WORD COUNT: intro paragraph (156); main text (2335)

129 **INTRODUCTORY PARAGRAPH**

130 Variation in body fat distribution contributes to the metabolic sequelae of obesity. The genetic
131 determinants of body fat distribution are poorly understood. The goal of this study was to gain
132 new insights into the underlying genetics of body fat distribution by conducting sample-size
133 weighted fixed-effects genome-wide association meta-analyses in up to 9,594 women and
134 8,738 men for six ectopic fat traits in European, African, Hispanic, and Chinese ancestry
135 populations, with and without sex stratification. In total, 7 new loci were identified in association
136 with ectopic fat traits (*ATXN1*, *UBE2E2*, *EBF1*, *RREB1*, *GSDMB*, *GRAMD3* and *ENSA*; $P < 5 \times 10^{-8}$;
137 $FDR < 1\%$). Functional analysis of these genes revealed that loss of function of both *ATXN1*
138 and *UBE2E2* in primary mouse adipose progenitor cells impaired adipocyte differentiation,
139 suggesting a physiological role for *ATXN1* and *UBE2E2* in adipogenesis. Future studies are
140 necessary to further explore the mechanisms by which these genes impact adipocyte biology
141 and how their perturbations contribute to systemic metabolic disease.

MAIN TEXT

Variation in body fat distribution is associated with cardiometabolic risk, including diabetes, hypertension and coronary heart disease,¹⁻⁵ and is at least partially independent of total adiposity. Adipose tissue can be quantified non-invasively using computed tomography (CT) and magnetic-resonance imaging (MRI) to measure fat volume and fat attenuation in different tissue compartments. We previously demonstrated that both indices, in addition to relative fat distribution, are important predictors of cardiometabolic risk.⁶⁻¹¹

Several lines of evidence suggest a unique genetic component to body fat distribution. First, indices of body fat distribution are heritable with values ranging from 36-47%, even after adjustment for body mass index (BMI).¹² Second, unique genetic loci exist for body fat distribution. For example, we identified a SNP associated with pericardial fat¹³ that was not associated with visceral fat,¹² BMI or waist-hip-ratio (WHR).^{14,15} Third, several lipodystrophy syndromes, characterized by abnormal body fat distribution, are genetically mediated.¹⁶

The current study presents a genome-wide association study and meta-analysis of adipose tissue traits derived from imaging biomarkers (Supplementary Table 1) from 2.6 million SNPs in up to 9,594 women and 8,738 men of European, African, Hispanic and Chinese ancestry (see Supplementary Tables 2, 3 and 4) and uses mouse models to characterize selected loci.

Subcutaneous and visceral adipose tissue (SAT, VAT) were previously estimated to have heritabilities of 57% and 36%, respectively^{12,17} (Supplementary Table 5). To assess the genetic contribution to variation in fat attenuation traits, which serve as indirect markers of fat quality (SAT Hounsfield Units [SATHU] and VATHU), heritability (H^2) was estimated in 3,312 women and men in the Framingham Heart Study (FHS), and found to be between 29-31% ($P < 1 \times 10^{-15}$). To assess the shared genetic contribution between ectopic fat traits, the genetic correlations were estimated among 3,336 women and men in FHS. Moderate to strong statistically significant correlations were observed between almost all ectopic fat traits pairs

(0.35 to 0.67 and -0.74 to -0.35, all $P < 5 \times 10^{-4}$; Supplementary Table 6), suggesting shared loci between ectopic fat traits. However, not all genes were shared between traits ($P < 5 \times 10^{-11}$ for non-overlapping correlations for all pairwise comparisons). The genetic correlations across the ectopic fat traits are also reflected in the phenotypic correlations (Supplementary Table 7).

In this combined multiethnic sample-size weighted fixed-effects meta-analysis^{18,19} of up to 18,332 participants, a total of 11 locus-trait associations (7 novel and 4 known) attained genome-wide significance ($P < 5 \times 10^{-8}$) out of 27 genomic scans (from analysis of 9 traits and models in 3 strata – overall, women and men). Of the 7 novel loci, 3 were associated with volumetric subcutaneous (*GSDMB*) and visceral fat traits (*GRAMD3* and *RREB1*), 2 were associated with pericardial fat (*ENSA* and *EBF1*), 1 was associated with fat attenuation (*ATXN1*), and 1 was associated with relative fat distribution (VAT/SAT ratio [*UBE2E2*]) (Table 1; Supplementary Figures 1a-g; with imputation quality in Supplementary Table 8). Associations were robust across ancestry-stratified sensitivity analyses (Supplementary Figures 2a-g and 3a-g; Supplementary Table 9). Manhattan plots and QQ plots for each analysis showed minimal inflation of association test statistics (Supplementary Figures 4a-g). The remaining 4 loci (*LYPLAL1*, *LY86*, *FTO*, *TRIB2*) attaining genome-wide significance were previously identified.^{12,13}

rs2123685, located between the 3' untranslated regions of *ZPBP2* and *GSDMB*, was associated with SAT in women only ($P_{\text{women}} = 3.4 \times 10^{-8}$, Supplementary Table 10a). Investigation of related ectopic traits among women revealed a direction-consistent nominal association with VAT ($P = 4.8 \times 10^{-4}$). SNPs at *FTO*, the canonical-BMI locus, attained genome-wide significance in association with SAT in the overall sample ($P = 1.4 \times 10^{-9}$).

The newly identified association at *RREB1* with VATadjBMI (rs2842895, $P = 1.1 \times 10^{-8}$) was observed in the overall sample and both sexes (Supplementary Table 10b). Examination of related ectopic traits demonstrated nominal associations with VAT and VAT/SAT ratio adjBMI ($P = 4.8 \times 10^{-5}$ and $P = 8.9 \times 10^{-6}$ respectively). The newly identified association of rs10060123 near

GRAMD3 for VATadjBMI was specific to women ($P=4.5 \times 10^{-8}$). This locus was nominally associated with VAT and VAT/SAT ratio adjBMI in women (Supplementary Table 10c).

PAT represents distinct ectopic fat deposition around the heart. Two findings in the overall sample at the *ENSA* and *EBF1* loci ($P=2.8 \times 10^{-9}$ and 1.0×10^{-9} , respectively, Table 1) have not been previously associated with ectopic fat, general adiposity or body fat distribution. Associations at *ENSA* and *EBF1* did not appear to be sex-specific (Supplementary Tables 10d and 10e). Further investigation of the *ENSA* and *EBF1* loci showed no associations with SAT, VAT or VAT/SAT ratio, underscoring their specificity to PAT. *TRIB2* was associated with PAT in this and our prior meta-analysis ($P < 5 \times 10^{-8}$).¹³

Cellular characteristics of fat quality, such as lipid content, vascularity, and adipocyte size and number, may be important factors influencing metabolic risk,^{7,10} but direct assessment is invasive. Fat attenuation traits, assessed with computed tomography, are correlated with fat quality characteristics^{20,21} and thus represent indirect markers of fat quality. *ATXN1* was associated with SATHU among men only ($P=1.4 \times 10^{-8}$) with no association among women ($P=0.36$, Supplementary Table 10f). Examination of related ectopic fat traits indicated similar direction of association with VATHU, and opposite direction for SAT and VAT (Supplementary Table 10f) which is consistent with epidemiology findings.⁷

The ratio of visceral to subcutaneous fat volumes (VAT/SAT ratio) represents the propensity to store fat viscerally. *UBE2E2* was associated with VAT/SAT ratio ($P=3.1 \times 10^{-10}$); a nominal association was also identified with VAT ($P=1.4 \times 10^{-3}$) but not SAT, suggesting the finding is mostly driven by the higher relative abundance of VAT. The direction of association in both sex strata was consistent (Supplementary Table 10g). Two known body fat distribution loci, *LYPLAL1* and *LY86*, were also associated with VAT/SAT ratio at genome-wide significance (Table 1), consistent with our prior analyses.^{12, 22}

Calculation of false discovery rate (FDR) to account for multiple testing across the 27 meta-analyses showed all ectopic fat loci that attained genome-wide significance in each individual GWAS ($P < 5 \times 10^{-8}$) also attained an $FDR < 1\%$.

To examine the association of the 7 newly identified ectopic fat loci with BMI and WHR, cross-trait evaluations for each lead SNP were performed in the most recent GIANT meta-GWAS, with sample sizes ~10-20 times larger than the current study.^{14,15} Only 2 out of 14 SNP-trait (BMI or WHR) associations were significant after Bonferroni correction for multiple testing ($P < 0.05/14 = 3.6 \times 10^{-3}$; Supplementary Table 10a-g), highlighting the specificity and uniqueness of the ectopic fat loci.

To evaluate the relationship between the known 97 BMI and 49 WHR loci^{14,15} and ectopic fat traits, we examined the association for these loci with fat volume and relative fat volume traits among the combined multiethnic sample of women and men. Because the ectopic fat data may be underpowered to determine statistically significant results, we hypothesized that the direction of the BMI and WHR findings would be directionally consistent with abdominal ectopic traits, even if the p-values were not significant (Supplementary Table 11). Direction consistent SNP-trait associations between SAT and BMI were observed for 87 of 97 loci ($P_{\text{binomial}} = 8.9 \times 10^{-17}$). When restricted to the 27 loci nominally associated with SAT ($P_{\text{SAT}} < 0.05$), all 27 SNP-SAT associations were directionally consistent with BMI ($P_{\text{binomial}} = 7.5 \times 10^{-9}$). SAT is not an ectopic fat depot and may represent a metabolic sink for healthier fat storage that is highly correlated with BMI and shares genetic risk factors (as shown with the enriched number of direction consistent associations), yet also represents a unique metric of fat distribution with unique genetic influences (as shown with the *GSDMB*-SAT association). No other traits showed directionally consistent associations with the BMI or WHR (all $P > 0.05$). These results further underscore how ectopic fat traits are uniquely disparate traits as compared to BMI and WHR.

Ectopic fat depots are associated with cardiometabolic risk and cardiovascular events.⁸⁻
¹¹ To gain insight into potential mechanisms linking these conditions, we evaluated the association of the new ectopic fat loci with traits from large-scale genetics consortia. Of 66 pairs of lead SNP-trait associations examined, 3 associations (*UBE2E2*-type 2 diabetes [T2D], *EBF1*-triglycerides, and *EBF1*-HDL cholesterol) were statistically significant after Bonferroni correction for multiple testing ($P < 0.05/66 = 8 \times 10^{-4}$; Supplementary Table 12).

To examine if any of the new variants overlap with known regulatory regions in adipose tissue, lead SNPs and variants in linkage disequilibrium (LD) with the lead SNPs ($r^2 > 0.8$) were interrogated using ENCODE Consortium data implemented in HaploReg²³ and RegulomeDB.²⁴ Except for *ATXN1*, all other loci contained SNPs in LD with the lead SNP that overlapped with known regulatory regions in adipose tissue. For example, the lead *UBE2E2* variant (rs7374732), and other SNPs in LD, overlapped with a known enhancer region in adipose derived stem cells (Supplementary Table 13).

The list of candidate loci was further prioritized based on visual examination of regional association plots (Supplementary Figures 1a-g) and identification of 1) a localized association within a gene body at each locus (*RREB1*, *ATXN1* and *UBE2E2*), or 2) a localized association near the gene body concomitant with the lack of other genes within 1Mbp of the lead SNP (*EBF1*). In applying these criteria, four genes were selected for additional functional study.

To test the hypothesis that inter-depot differences in gene expression or their dynamic regulation during adipocyte development would identify candidates with a higher likelihood of functional significance, expression of 4 genes (*Ebf1*, *Rreb1*, *Atxn1*, *Ube2e2*) in murine SAT, VAT, and PAT depots was assessed by qPCR. *Ube2e2* was expressed more highly in the perigonadal VAT of 6 week-old C57BL/6 mice relative to the SAT (2.1 fold, $p < 0.05$, $n = 5$) or PAT (2.6 fold, $p < 0.01$, $n = 5$), but no differences were observed for *Ebf1*, *Rreb1* or *Atxn1* (Figure 1a). Differential gene expression of these 4 genes was also assessed in murine diet-induced obesity. A 2.1 fold induction of *Atxn1* expression in SAT of diet-induced obese mice was

observed relative to lean controls ($p < 0.05$, $n = 6$). Significant differences were not observed for *Ebf1*, *Rreb1*, or *Ube2e2* in response to the obesogenic stimulus (Figure 1b).

To explore a potential role for the candidate genes in adipocyte development, we examined their regulation during *ex vivo* adipogenic differentiation of progenitor-rich stromal-vascular cell fractions isolated from the subcutaneous and visceral depots of C57BL/6 mice. Candidate gene expression was measured at regular intervals during adipogenic differentiation. In progenitors isolated from both VAT and SAT, we observed a significant down-regulation of *Atxn1*, *Ube2e2*, and *Ebf1* during adipogenesis (Figure 1c and Supplementary Figure 5). However, in all three instances the expression returned to near baseline levels by 96h post-adipogenic induction. In contrast, no significant transcriptional regulation of *Rreb1* after adipogenic induction was observed (Supplementary Figure 5).

Both *Atxn1* and *Ube2Ee2* showed evidence of dynamic regulation of gene expression during adipogenesis with variable depot-specific expression in the murine models providing rationale to further explore their functional significance with a genetic loss-of-function assay. Knock-down of both genes with specific shRNA retroviral constructs during *ex vivo* adipogenesis of SAT progenitors impaired the formation of lipid-containing adipocytes relative to vector control infected cells, whereas only *Ube2e2* knock-down impaired adipogenesis in progenitors isolated from VAT (Figure 1d,e).

Our findings provide insight into the genetics of body fat distribution. The scant number of significant associations observed between the ectopic fat loci and more general measures of adiposity, such as BMI and WHR,^{14,15} demonstrates the specificity of the ectopic fat associations, highlights the utility of precise phenotyping of fat distribution, and suggests different mechanisms involved in ectopic fat storage compared to more general adiposity measures. This specificity was particularly notable for PAT loci, which demonstrate no associations with SAT, VAT, VAT/SAT ratio, BMI or WHR.

In addition, few cross-trait associations were observed for ectopic fat loci and other cardiometabolic traits, which is striking given the epidemiologic associations between ectopic fat and cardiometabolic risk¹⁻⁵. One notable exception is *UBE2E2*, which is a known T2D locus^{25,26}. The lead T2D SNP does not appear to be in LD with the lead SNP from our study (r^2 [rs7374732, rs7612463]<0.08 across all HapMap2 populations), and therefore likely represents an independent signal. The major allele at rs7374732 is associated with both lower VAT/SAT ratio and lower risk of T2D, suggesting that targeting relative fat distribution may have beneficial downstream effects.

Functional studies support a physiologic role for *UBE2E2* and *ATXN1* through regulation of adipocyte differentiation. *ATXN1* encodes a chromatin binding factor involved in the repression of Notch signaling. It has been implicated in neurologic diseases, including spinocerebellar ataxia 1, but there are no reported associations between SNPs in *ATXN1* and adiposity-related traits. In contrast, *UBE2E2* is a known T2D GWAS locus,²⁵⁻²⁷ although the markers are in low LD with the lead SNP in the present study. *UBE2E2* (3p24.2) encodes the ubiquitin-conjugating enzyme E2E2, which is expressed in human pancreas, liver, muscle and adipose tissues. The present GWAS results highlight *UBE2E2* in association with the VAT/SAT ratio, a measure of the relative propensity to store fat in the visceral cavity rather than the subcutaneous compartment. We therefore speculate that SNP-associated modulation of gene expression or function of the protein products may impact adiposity through an effect on adipocyte differentiation and relative impairments in adipocyte development may partially explain a default propensity to deposit viscerally as compared to subcutaneously.

Given the uniqueness of the ectopic fat traits, the sample size was limited in comparison to other meta-analyses. Moreover, identification of candidate genes based on proximity to a GWAS signal may miss long distance interactions between genes and regulatory domains. In contrast, multiethnic analyses, such as this study, not only enhance generalizability, but may also boost power for certain traits, particularly in contexts of limited allelic heterogeneity. The

possibility of false positive loci is also a consideration, given the absence of external replication. However, all newly identified loci passed $FDR < 1\%$. Such statistical limitations are further mitigated in the case of *ATXN1* and *UBE2E2* by functional validation of these loci in murine adipose tissue.

Combining large-scale discovery human genetics with the detailed fat phenotyping and experiments in model organisms identified 7 new loci in association with ectopic fat traits, of which *ATXN1* and *UBE2E2* demonstrated a functional effect during adipocyte differentiation. Future studies should further explore the exact mechanism by which modulation of *ATXN1* and *UBE2E2* impact adipocyte differentiation and whether this effect causally impacts systemic metabolic disease.

Data availability statement: Summary statistics for all meta-analyses will be made available at the following website <https://www.nhlbi.nih.gov/research/intramural/researchers/ckdgen>.

Acknowledgements: Please see Supplementary Note for Acknowledgments and Funding Sources.

Author contributions

Study design: X Guo, AH Kissebah, J Kullberg, LJ Launer, M Olivier, PA Peyser, IB Borecki, DW Boden, SA Czerwinski, J Ding, V Gudnason, TB Harris, C Langefeld, L Lind, Y Liu, JI Rotter, B Towne, M Allison

Study management: Yi Zhang, LJ Launer, M Olivier, PA Peyser, JG Terry, IB Borecki, DW Boden, JJ Carr, SA Czerwinski, V Gudnason, TB Harris, L Lind, BD Mitchell, TH Mosely, Jr, JI Rotter, AR Shuldiner, H Völzke, JG Wilson, M Allison

Subject recruitment: AH Kissebah, J Kullberg, MK Wojczynski, DW Boden, SA Czerwinski, V Gudnason, L Lind, BD Mitchell, TH Mosely, Jr, AR Shuldiner, B Towne, H Völzke

Interpretation of results: AY Chu, X Deng, VA Fisher, Yang Zhang, MF Feitosa, C Liu, O Weeks, AC Choh, Q Duan, X Guo, NL Heard-Costa, X Liu, L Lu, JR O'Connell, A Parihar, AV Smith, Yi Zhang, AH Kissebah, M Olivier, PA Peyser, JG Terry, MK Wojczynski, LF Bielak, IB Borecki, DW Boden, JJ Carr, SA Czerwinski, J Ding, N Friedrich, SL Kardia, C Langefeld, Y Liu, BD Mitchell, JI Rotter, AR Shuldiner, B Towne, H Wallaschofski, M Allison, CM Lindgren, W Goessling, LA Cupples, ML Steinhauser, CS Fox

Drafting manuscript: AY Chu, Yang Zhang, MF Feitosa, X Guo, JW Kent Jr., Yi Zhang, AH Kissebah, MK Wojczynski, IB Borecki, CM Lindgren, ML Steinhauser, CS Fox

Critical review: AY Chu, X Deng, VA Fisher, MF Feitosa, C Liu, O Weeks, AC Choh, X Guo, NL Heard-Costa, JW Kent Jr., X Liu, L Lu, A Mahajan, JR O'Connell, A Parihar, Yi Zhang, G Homuth, AH Kissebah (deceased), J Kullberg, M Nauck, M Olivier, PA Peyser, JG Terry, LF

358 Bielak, J Blangero, IB Borecki, DW Boden, JJ Carr, SA Czerwinski, J Ding, N Friedrich, E
 359 Ingelsson, SL Kardia, C Langefeld, L Lind, Y Liu, BD Mitchell, AP Morris, TH Mosely, Jr, JI
 360 Rotter, AR Shuldiner, B Towne, H Völzke, H Wallaschofski, M Allison, CM Lindgren, W
 361 Goessling, LA Cupples, ML Steinhauser, CS Fox
 362 **Statistical methods and analysis:** AY Chu, X Deng, VA Fisher, A Drong, Yang Zhang, MF
 363 Feitosa, AC Choh, Q Duan, TD Dyer, JD Eicher, X Guo, NL Heard-Costa, T Kacprowski, JW
 364 Kent Jr., LA Lange, X Liu, K Lohman, L Lu, A Mahajan, JR O'Connell, A Parihar, JM Peralta, AV
 365 Smith, J Yao, LF Bielak, J Ding, C Langefeld, Y Liu, BD Mitchell, AP Morris, CM Lindgren
 366 **Genotyping:** Yi Zhang, G Homuth, M Olivier, DW Boden, SA Czerwinski, E Ingelsson, SL
 367 Kardia, Y Liu, AP Morris, JI Rotter, AR Shuldiner, B Towne, CM Lindgren
 368 **Bioinformatics:** AY Chu, X Deng, VA Fisher, MF Feitosa, C Liu, AC Choh, JD Eicher, AD
 369 Johnson, T Kacprowski, AV Smith, Yi Zhang
 370 **Data collection:** Yang Zhang, O Weeks, R Laqua, N Friedrich, W Goessling, ML Steinhauser
 371 **Animal work/functional data:** Yang Zhang, ML Steinhauser
 372
 373 **Disclosures:** Caroline S. Fox and Audrey Y. Chu are employed by Merck Research
 374 Laboratories as of December 14, 2015 and July 18, 2016, respectively.
 375
 376 **Disclaimer:** The views expressed in this manuscript are those of the authors and do not
 377 necessarily represent the views of the National Heart, Lung, and Blood Institute; the National
 378 Institutes of Health; or the U.S. Department of Health and Human Services. Please see
 379 Supplementary Note for acknowledgements and funding sources.
 380
 381

382 REFERENCES

- 383 1. Ding, J. *et al.* The association of regional fat depots with hypertension in older persons
384 of white and African American ethnicity. *Am. J. Hypertens.* **17**, 971-976,
385 doi:10.1016/j.amjhyper.2004.05.001 (2004).
- 386 2. Goodpaster, B. H. *et al.* Association between regional adipose tissue distribution and
387 both type 2 diabetes and impaired glucose tolerance in elderly men and women.
388 *Diabetes Care* **26**, 372-379 (2003).
- 389 3. Hayashi, T. *et al.* Visceral adiposity is an independent predictor of incident hypertension
390 in Japanese Americans. *Ann. Intern. Med.* **140**, 992-1000 (2004).
- 391 4. Kanaya, A. M. *et al.* Adipocytokines attenuate the association between visceral adiposity
392 and diabetes in older adults. *Diabetes Care* **27**, 1375-1380 (2004).
- 393 5. Nicklas, B. J. *et al.* Visceral adipose tissue cutoffs associated with metabolic risk factors
394 for coronary heart disease in women. *Diabetes Care* **26**, 1413-1420 (2003).
- 395 6. Kaess, B. M. *et al.* The ratio of visceral to subcutaneous fat, a metric of body fat
396 distribution, is a unique correlate of cardiometabolic risk. *Diabetologia* **55**, 2622-2630,
397 doi:10.1007/s00125-012-2639-5 (2012).
- 398 7. Rosenquist, K. J. *et al.* Visceral and subcutaneous fat quality and cardiometabolic risk.
399 *JACC Cardiovasc. Imaging* **6**, 762-771, doi:10.1016/j.jcmg.2012.11.021 (2013).
- 400 8. Britton, K. A. *et al.* Body fat distribution, incident cardiovascular disease, cancer, and all-
401 cause mortality. *J. Am. Coll. Cardiol.* **62**, 921-925, doi:10.1016/j.jacc.2013.06.027
402 (2013).
- 403 9. Alvey, N. J. *et al.* Association of fat density with subclinical atherosclerosis. *J Am Heart*
404 *Assoc* **3**, doi:10.1161/JAHA.114.000788 (2014).
- 405 10. Rosenquist, K. J. *et al.* Fat quality and incident cardiovascular disease, all-cause
406 mortality, and cancer mortality. *J. Clin. Endocrinol. Metab.* **100**, 227-234,
407 doi:10.1210/jc.2013-4296 (2015).
- 408 11. Abraham, T. M., Pedley, A., Massaro, J. M., Hoffmann, U. & Fox, C. S. Association
409 Between Visceral and Subcutaneous Adipose Depots and Incident Cardiovascular
410 Disease Risk Factors. *Circulation* **132**, 1639-1647,
411 doi:10.1161/CIRCULATIONAHA.114.015000 (2015).
- 412 12. Fox, C. S. *et al.* Genome-wide association for abdominal subcutaneous and visceral
413 adipose reveals a novel locus for visceral fat in women. *PLoS genetics* **8**, e1002695,
414 doi:10.1371/journal.pgen.1002695 (2012).
- 415 13. Fox, C. S. *et al.* Genome-wide association of pericardial fat identifies a unique locus for
416 ectopic fat. *PLoS genetics* **8**, e1002705, doi:10.1371/journal.pgen.1002705 (2012).
- 417 14. Shungin, D. *et al.* New genetic loci link adipose and insulin biology to body fat
418 distribution. *Nature* **518**, 187-196, doi:10.1038/nature14132 (2015).
- 419 15. Locke, A. E. *et al.* Genetic studies of body mass index yield new insights for obesity
420 biology. *Nature* **518**, 197-206, doi:10.1038/nature14177 (2015).
- 421 16. Almasy, L. & Blangero, J. Multipoint quantitative-trait linkage analysis in general
422 pedigrees. *Am. J. Hum. Genet.* **62**, 1198-1211, doi:10.1086/301844 (1998).
- 423 17. Fox, C. S. *et al.* Abdominal visceral and subcutaneous adipose tissue compartments:
424 association with metabolic risk factors in the Framingham Heart Study. *Circulation* **116**,
425 39-48, doi:10.1161/CIRCULATIONAHA.106.675355 (2007).
- 426 18. Willer, C. J., Li, Y. & Abecasis, G. R. METAL: fast and efficient meta-analysis of
427 genomewide association scans. *Bioinformatics* **26**, 2190-2191,
428 doi:10.1093/bioinformatics/btq340 (2010).
- 429 19. Stouffer, S. A., Suchman, E. A., DeVinney, L. C., Star, S. A. & Williams, R. M. J.
430 *Adjustment During Army Life.* (Princeton University Press, 1949).

20. Baba, S., Jacene, H. A., Engles, J. M., Honda, H. & Wahl, R. L. CT Hounsfield units of brown adipose tissue increase with activation: preclinical and clinical studies. *J. Nucl. Med.* **51**, 246-250, doi:10.2967/jnumed.109.068775 (2010).
21. Hu, H. H., Chung, S. A., Nayak, K. S., Jackson, H. A. & Gilsanz, V. Differential computed tomographic attenuation of metabolically active and inactive adipose tissues: preliminary findings. *J. Comput. Assist. Tomogr.* **35**, 65-71, doi:10.1097/RCT.0b013e3181fc2150 (2011).
22. Heid, I. M. *et al.* Meta-analysis identifies 13 new loci associated with waist-hip ratio and reveals sexual dimorphism in the genetic basis of fat distribution. *Nat. Genet.* **42**, 949-960, doi:10.1038/ng.685 (2010).
23. Ward, L. D. & Kellis, M. HaploReg: a resource for exploring chromatin states, conservation, and regulatory motif alterations within sets of genetically linked variants. *Nucleic Acids Res.* **40**, D930-934, doi:10.1093/nar/gkr917 (2012).
24. Boyle, A. P. *et al.* Annotation of functional variation in personal genomes using RegulomeDB. *Genome Res.* **22**, 1790-1797, doi:10.1101/gr.137323.112 (2012).
25. Replication, D. I. G. *et al.* Genome-wide trans-ancestry meta-analysis provides insight into the genetic architecture of type 2 diabetes susceptibility. *Nat. Genet.* **46**, 234-244, doi:10.1038/ng.2897 (2014).
26. Yamauchi, T. *et al.* A genome-wide association study in the Japanese population identifies susceptibility loci for type 2 diabetes at UBE2E2 and C2CD4A-C2CD4B. *Nat. Genet.* **42**, 864-868, doi:10.1038/ng.660 (2010).
27. Hara, K. *et al.* Genome-wide association study identifies three novel loci for type 2 diabetes. *Hum. Mol. Genet.* **23**, 239-246, doi:10.1093/hmg/ddt399 (2014).

FIGURE LEGEND

Figure 1. Functional characterization of *Atxn1*, *Ebf1*, *Rreb1* and *Ube2e2*.

(a,b,e) Data is displayed as box/whisker plots where the center line represents the median, box limits contain the 25th-75th percentiles, and whiskers span max/min values.

(a) Gene expression measured by qPCR in murine subcutaneous (SAT), perigonadal visceral (VAT), and pericardial (PAT) adipose tissues (n=6 mice). Statistical significance was assessed using ANOVA and Sidak's correction for multiple comparisons.

(b) Gene expression measured by qPCR in murine adipose tissues after 8 weeks of high fat feeding compared to normal chow fed controls (n=5 mice per group). Statistical significance was assigned using a two-sided T-test.

(c) Gene expression measured by qPCR in cultured adipocyte progenitors isolated from the subcutaneous (SAT) or perigonadal visceral (VAT) depots (n=4 replicates). Cells were expanded to confluence and then collected at intervals after induction of adipogenic differentiation. Data displayed as mean, error bar=s.e.m. Statistical significance was assessed using ANOVA and Sidak's correction for multiple comparisons to time 0.

(d) Oil-red-o staining of progenitors isolated from subcutaneous adipose and exposed to retroviral delivery of shRNA constructs during *ex vivo* expansion and induction of adipogenesis. Relative to control vector carrying a scramble sequence, shRNA constructs specific for *Atxn1* and *Ube2e2* impaired adipogenic differentiation. Scale=1mm.

(e) Oil-red-o stain was alcohol extracted and quantified at OD₅₂₀ (n=9 technical replicates). Statistical significance was assessed using ANOVA and Sidak's correction for multiple comparisons to control (Scramble). Data representative of 3 independent experiments.

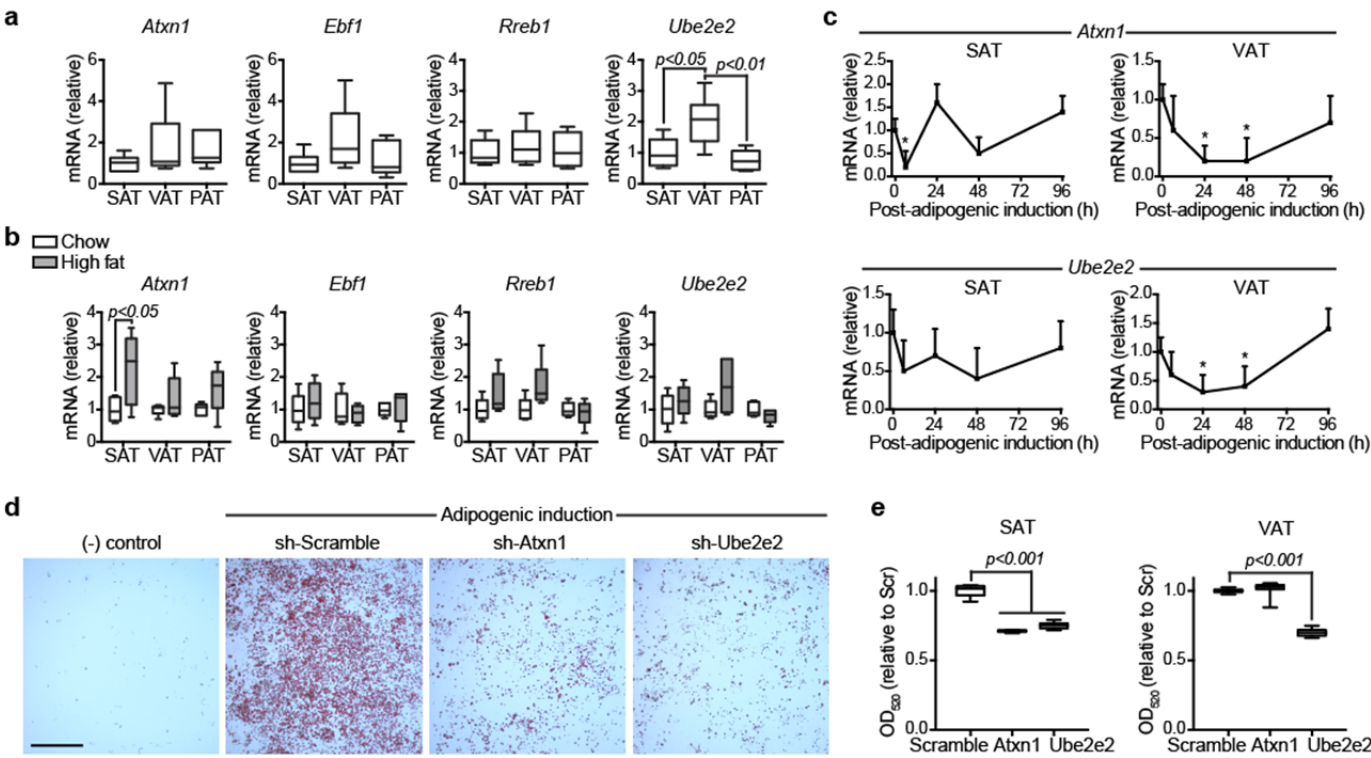
478 **Table 1.** SNPs associated with ectopic fat traits ($p < 5 \times 10^{-8}$)¹. Association statistics were obtained using a sample-size weighted fixed-
479 effects meta-analysis implemented in METAL.^{18,19}

	Locus ²	Trait	Strata	Lead SNP	Chr	SNPID	Position	A1 ³	A2 ⁴	Freq A1 ⁵	N	Z score	P-value ⁶
Fat Volume Traits ^{7,8}													
NEW													
	ENSA	PATadjHtWt	ALL	rs6587515	1	rs6587515	148875512	a	g	0.09	11027	-5.94	2.8x10 ⁻⁹
	GRAMD3	VATadjBMI	WOMEN	rs10060123	5	rs10060123	125711809	a	c	0.23	9623	5.47	4.5x10 ⁻⁸
	EBF1	PATadjHtWt	ALL	rs1650505	5	rs1650505	157962312	a	g	0.24	11566	-6.10	1.0x10 ⁻⁹
		PAT	ALL		5	rs2434264	157954781	t	g	0.61	11614	5.93	3.0x10 ⁻⁹
	RREB1	VATadjBMI	ALL	rs2842895	6	rs2842895	7051315	c	g	0.50	17297	5.72	1.1x10 ⁻⁸
	GSDMB	SAT	WOMEN	rs2123685	17	rs2123685	35307415	t	c	0.94	7137	5.52	3.4x10 ⁻⁸
KNOWN													
	TRIB2	PATadjHtWt	ALL	rs10198628	2	rs10198628	12881948	a	g	0.42	11572	-8.88	6.7x10 ⁻¹⁹
		PATadjHtWt	MEN							0.43	5466	-6.68	2.4x10 ⁻¹¹
		PATadjHtWt	WOMEN							0.42	6106	-6.02	1.8x10 ⁻⁹
		PAT	ALL							0.42	11605	-7.87	3.7x10 ⁻¹⁵
	FTO	SAT	ALL	rs7185735	16	rs7185735	52380152	a	g	0.58	17812	-6.05	1.4x10 ⁻⁹
Fat Attenuation Traits ^{7,8}													
NEW													
	ATXN1	SATHU	MEN	rs2237199	6	rs2237199	16538000	a	g	0.11	5780	5.67	1.4x10 ⁻⁸
Relative Fat Distribution Traits ^{7,8}													
NEW													
	UBE2E2	VAT/SAT ratio	ALL	rs7374732	3	rs7374732	23178458	t	c	0.69	18205	-6.29	3.1x10 ⁻¹⁰
		VAT/SAT ratio adjBMI	ALL							0.69	18190	-5.64	1.7x10 ⁻⁸
KNOWN													
	LYPLAL1	VAT/SAT ratio	ALL	rs6689335	1	rs6689335	217695305	t	c	0.59	15214	-5.59	2.3x10 ⁻⁸
		VAT/SAT ratio adjBMI	ALL		1	rs6689335	217695305	t	c	0.59	15199	-5.53	3.2x10 ⁻⁸
	LY86	VAT/SAT ratio	ALL	rs912056	6	rs912056	6681196	a	t	0.35	17387	-5.96	2.5x10 ⁻⁹
		VAT/SAT ratio adjBMI	ALL							0.35	17372	-5.98	2.3x10 ⁻⁹

480 ¹ SNPs are grouped by ectopic fat trait and are listed by new discoveries and then previously identified loci. Any association attaining
481 genome-wide significance ($p < 5 \times 10^{-8}$) is listed.

482 ² Conventional locus name based on closest gene in the region
483 ³ A1 is the coded allele
484 ⁴ A2 is the non-coded allele
485 ⁵ FreqA1 is the allele frequency of Allele1
486 ⁶ P-values are double genomic control corrected
487 ⁷ European and African ancestry cohorts contributed to all ectopic fat traits; Chinese and Hispanic ancestry cohorts contributed only
488 to pericardial volume traits
489 ⁸ Abbreviations:
490 SAT - Subcutaneous Adipose Tissue Volume
491 VAT - Visceral Adipose Tissue Volume
492 PAT - Pericardial Adipose Tissue Volume
493 SATHU - Subcutaneous Adipose Tissue Attenuation
494 VATHU - Visceral Adipose Tissue Attenuation
495 VAT/SAT ratio - Visceral to Subcutaneous Adipose Tissue Volume Ratio
496 adjBMI - Model Adjusted for BMI
497 adjHtWt - Model Adjusted for Height and Weight

498 **Figure 1.**



499

Online Methods

Study Participants

Up to 18,332 participants from 13 cohorts of European and African ancestry were available for analysis of subcutaneous and visceral adipose tissue volumetric traits, up to 11,596 from 6 cohorts of European, African, Asian, and Hispanic ancestry were available for analysis of pericardial adipose volumetric traits, up to 12,519 participants from 5 cohorts of European and African ancestry were available for analysis of attenuation traits, and up to 18,191 participants from 6 cohorts of European and African ancestry were available for analysis of relative fat distribution traits. This epidemiological sample constitutes the largest known collection of participants with radiologically derived ectopic fat measures and genetic data at the inception of this project. Supplementary Table 2 and 3 contain information regarding imaging modality used by each cohort, distribution by sex and ancestry per cohort for each trait analyzed and cohort descriptive information. All participants provided informed consent and each study was approved by their governing ethics committee.

Trait assessment

The traits measured in this study can be categorized into three groups: 1) fat volume measurements: subcutaneous adipose tissue (SAT), visceral adipose tissue (VAT) and pericardial adipose tissue (PAT); 2) fat attenuation measurements: subcutaneous adipose tissue attenuation (SATHU) and visceral adipose tissue attenuation (VATHU); and 3) relative fat distribution measurements: visceral-to-subcutaneous adipose tissue volume ratio (VAT/SAT ratio). All volume-based measures were assessed by computed tomography (CT) or magnetic resonance imaging (MRI) following study-specific protocols; attenuation-based measures were assessed by CT following study specific protocols. Please see Supplementary Table 2 and Supplementary Note for further detail.

The following traits were created by each cohort in the overall sample, women and men: volume-based traits - SAT, VAT, VAT adjusted for BMI, PAT, PAT adjusted for height and weight; attenuation-based traits - SATHU and VATHU; relative-distribution traits - VAT/SAT ratio, VAT/SAT ratio adjusted for BMI pericardial traits. The rationale for including the ectopic fat traits, the adjustment models, and the sex-stratified analyses was 4-fold. First, ectopic fat measures are correlated with each other and with general adiposity and we wished to adjust for these factors as potential confounders or intermediates and to examine the genetic associations independent of the adjustment factor. Please see refer to Supplementary Table 7 for pairwise correlations of all traits within FHS, the largest participating cohort. For example, the correlation between VAT and BMI is 0.71 to 0.75 and adjusting for BMI when examining VAT provides the relative amount of VAT controlling for degree of general adiposity. Although the correlations between VAT/SAT ratio and BMI are modest, adjusting for BMI allowed us to examine the propensity to store fat viscerally compared to subcutaneously independent of general adiposity. Second, adjustment of covariates reduces the residual variance of the trait associated with the given covariate and thus increases power to detect genetic associations. Third, in the adiposity genetics literature there is evidence of sexually dimorphic loci in which the variance explained is larger in women versus men²⁸ and association of the loci is markedly stronger in women compared to men, and vice versa.^{14,22} Lastly, we adjusted PAT for height and weight to be consistent with our prior work¹³ (see Supplementary Table 1 for guide to nomenclature for traits and adjustment models).

Due to the known differences in body fat distribution by sex, each cohort created sex- and ancestry-specific residuals adjusted for age, age-squared, smoking status, measures of subpopulation stratification and family structure (if necessary). Family-based studies created an additional set of residuals from all participants (both women and men) to account for family structure when analyzing the overall sample. Participants with missing genotype, phenotype or covariate data were excluded from analysis as pre-specified in the analysis plan.

Study Specific Protocol

Trait measurements and descriptions from each cohort are available in Supplementary Material under “Cohort Specific Information and Protocols”.

Genotyping and Imputation

Each cohort was genotyped as specified in Supplementary Table 4 and performed ancestry-specific imputation up to ~2.6 million SNPs based on the HapMap Project Phase 2 haplotypes (<http://hapmap.ncbi.nlm.nih.gov/index.html.en>). All newly identified loci were imputed with imputation qualities >0.8 in each cohort. Imputation quality by locus and cohort are available in Supplementary Table 8.

Heritability Analysis

Heritability was estimated from the Framingham Heart Study using variance components analysis in SOLAR.¹⁶

Genetic Correlation Analysis

Pairwise genetic correlations between subcutaneous fat (volume and attenuation), visceral fat (volume and attenuation), ratio of visceral-to-subcutaneous fat and BMI were calculated using SOLAR¹⁶ in the Framingham Heart Study among 3,312 participants. We used residuals adjusted for age and sex. Two separate hypotheses were tested: 1) $RhoG=0$ is the test for overlapping genetic correlations, and 2) absolute value ($RhoG$)=1 is the test for non-overlapping genetic correlations.

Statistical Analysis

Within each cohort, by ancestry and by sex, genome-wide linear regression analyses were conducted on the 11 trait and model combinations assuming an additive genetic model

using allele dosages. All traits approximated a normal distribution and untransformed traits were used for analysis. To prevent the undue influence of rare variants and/or of poorly imputed SNPs, we included variants with a minor allele count >10 and imputation quality >0.4 (for MaCH²⁹) or >0.3 (for IMPUTE³⁰) in each cohort.

For multiethnic analysis, we combined all cohort-specific results using a sample size-weighted fixed-effects meta-analysis (Stouffer's method) as implemented in METAL^{18,19} to allow for differences in trait measurement and scaling due to different imaging modalities across cohorts. European and African ancestry cohorts contributed to all ectopic fat traits; Chinese and Hispanic ancestry cohorts contributed only to pericardial volume traits (Supplementary Table 3). All analyses were performed for the overall sample (ALL), among women only (WOMEN) and among men only (MEN). All analyses were corrected for genomic control at the cohort-level. We excluded variants with minor allele frequency (MAF)<5% due to the low power to detect associations of such variants. We set a traditional genome-wide significance threshold at $P<5\times 10^{-8}$, the Bonferroni correction for the number of independent and common variants across the genome (~1 million SNPs). All p-values represent two-sided p-values unless otherwise specified. All regional association plots, Manhattan plots, and QQ plots were created using R version 3.1.1 (<https://cran.r-project.org/>). Linkage disequilibrium plots were created using SNAP³¹ and the gap R package (<https://www.jstatsoft.org/article/view/v023i08>).

To correct for multiple testing, false discovery rate (FDR) was calculated across the 27 ectopic fat GWAS scans using the qvalue R package (<http://github.com/jdstorey/qvalue>). FDR<1% was set as the multiple testing corrected significance threshold.

For mouse studies, individual cages of mice were randomly assigned in an un-blinded fashion to normal chow or high fat diet. Each *in vivo* study was conducted one time and no mice were excluded from the analyses. In the absence of *a priori* data regarding the variance of gene expression in the tissues of interest, we applied sample sizes that have in our experience been of sufficient size to detect a two-fold increase in gene expression. For normally distributed data

from more than two groups (Shapiro-Wilk), an ANOVA test followed by Sidak's correction for multiple testing was conducted (Figures 1a,c,e). For non-normal data a Kruskal-Wallis test was used. For comparisons between two normally distributed groups (Figure 1b: chow versus high fat) a two-sided T-test was used, unless the data was non-normal, in which case a Mann-Whitney test was used. Data were expressed as mean, s.e.m. Significance was assigned for two-sided $p < 0.05$. Data were analyzed and graphed using JMP 10.0 (SAS institute) and Prism 6 (Graphpad).

Sensitivity Analyses

To ensure the newly identified loci from our multiethnic analysis were robust and not driven by statistical outliers related to ancestry, ancestry-specific meta-analysis results were compared with each other with respect to the minor allele, the minor allele frequency and direction of the Z-score association statistic (Supplementary Table 9). Due to the scaling differences in imaging modalities across each cohort and use of the sample size weighted meta-analysis heterogeneity statistics cannot be calculated.

The lead SNP for the *GSDMB* locus associated with SAT in women was not observed in non-European ancestry cohorts and thus was not included in this analysis. For each of the remaining 6 lead SNPs from the newly identified ectopic fat loci, Z scores were directionally consistent across ancestry-specific meta-analyses (please see Supplementary Figure 2 for forest plots of each locus and Supplementary Figure 3 for linkage disequilibrium [LD] plots across ancestry). For 5 of these loci, the minor allele was identical across ancestries; only the minor allele of rs2842895 (*RREB1*) differed between the European ancestry and African ancestry cohorts. This observation may explain the slight attenuation in the association of *RREB1* and VATadjBMI after combining European and African ancestries in the multiethnic meta-analysis ($P_{\text{European-ancestry}} = 5.8 \times 10^{-9}$ to $P_{\text{multiethnic}} = 1.1 \times 10^{-8}$), although the multiethnic result remains genome-wide significant.

Analyses of Related Traits

For each SNP attaining genome-wide significance in association with any ectopic fat trait, we extracted association results in each strata of analysis (ALL, WOMEN, and MEN) for related ectopic fat traits within our study.

To investigate the association of the new ectopic fat loci with measures of generalized adiposity (BMI) and central obesity (WHR) - two traits that are strongly correlated with, but distinct from ectopic fat - we evaluated the lead genome-wide significant SNPs in publically available datasets from the most recent GIANT meta-analyses of BMI and WHR.^{14,15}

To investigate associations of new loci with cardio-metabolic traits that are epidemiologically associated with ectopic fat, cross-trait evaluations for the lead SNPs only were performed in the publically available datasets from the MAGIC (Meta-Analyses of Glucose and Insulin Consortium for fasting glucose and insulin³²), GLGC (Global Lipids Genetics Consortium for high-density lipoprotein cholesterol, triglycerides and total cholesterol³³), CARDIoGRAM+CAD consortium (Coronary ARtery Disease Genome wide Replication and Meta-analysis [CARDIoGRAM] plus The Coronary Artery Disease [C4D] Genetics for coronary artery disease and myocardial infarction^{34,35}), ICBP (International Consortium for Blood Pressure for systolic and diastolic blood pressure³⁶), and DIAGRAM (DIAbetes Genetics Replication And Meta-analysis²⁵).

Analysis of general adiposity and central adiposity loci

To evaluate the relationship between the known 97 BMI and 49 WHR loci^{14,15} with ectopic fat traits, we examined the association for these loci with fat volume and relative fat volume traits among the combined multiethnic sample of women and men. Because the ectopic fat data may be underpowered to determine statistically significant results, we hypothesized that the direction of the BMI and WHR findings would be directionally consistent with the ectopic fat traits, even if the p-values were not significant. Binominal tests were used to test the

significance of direction consistent associations (1-sided p-values). If the binominal test across the BMI or WHR loci was significant, a second 1-sided binominal test was performed evaluating consistency of associations restricting to SNPs with nominally significant associations ($P < 0.05$).

Functional Profiling - Bioinformatics and Annotation

To further characterize novel genome-wide significant loci, the following bioinformatics databases were queried for the lead ectopic fat loci: GWAS Catalog (<https://www.ebi.ac.uk/gwas/>; access date: 10/15/2015) to investigate other traits associated with newly identified loci, and HaploReg²³ and RegulomeDB²⁴ to identify regulatory elements overlapping the loci for the index SNP and SNPs in LD with the index SNP ($r^2 > 0.8$; Supplementary Table 13). To contextualize the newly identified ectopic loci and the surrounding genes, SNIPPER (<https://github.com/welchr/Snipper.git>) was used to search for biologically relevant mechanisms (Supplementary Table 14).

Variance Explained

The variance explained for each of the loci was approximated using the following formula $R^2 = \beta^2 \text{var}(\text{SNP}) / \text{var}(\text{ectopic fat trait})$, where β^2 is the estimated effect of the SNP on the ectopic fat trait, and $\text{var}(\text{SNP}) = 2 * \text{MAF}_{\text{SNP}} * (1 - \text{MAF}_{\text{SNP}})$. Because sample-size weighted fixed-effect meta-analysis does not estimate effect sizes, the beta-coefficient for the association between the SNP and ectopic fat trait and the variance of the ectopic fat trait were obtained from cohort level analysis per contributing study. The mean of the variance explained per locus across all contributing cohorts ranges from 0.1% to 4.4% (Supplementary Table 15).

Power Calculations

Power for discovery in the ectopic fat genomewide scan was calculated using GWAPower³⁷ using the range of sample size in this study (5,842-18,332 participants) and setting $\alpha = 5 \times 10^{-8}$. For the smallest sample size analyzed (N=5,842) we had $\geq 80\%$ power to detect loci explaining at least 0.64% of the trait variance. For the largest sample size analyzed (N=18,332), we had $\geq 80\%$ power to detect loci explaining at least 0.20% of the trait variance. For example, our novel loci explained from 0.15-4.4% of the trait variance for ectopic fat as seen in Supplementary Table 15.

To address the power to detect associations for the lookup analyses, we used GWAPower³⁷ with the maximum sample sizes from the each of the quantitative trait datasets (52,000-94,000 participants), a modest range of variance explained (0.01-0.05%; based on the variance explained for each locus [0.1-4.4%] and the age- adjusted correlations between ectopic fat and the cardiometabolic trait of interest [$R^2=0.02-0.46$]) and a Bonferroni corrected $\alpha = 7.4 \times 10^{-4}$ ($\sim 0.05/66$ pairs of SNP-trait associations). For the smallest dataset (Fasting Insulin, N~52,000), we had 80% power to detect loci explaining at least 0.030% of the variance in fasting insulin. For the largest dataset (HDL-C and total cholesterol, N~94,000), we had 80% power to detect loci explaining 0.018% of the variance in HDL-C or total cholesterol. These calculations indicate that we largely had adequate power for a large portion of the SNP-trait associations.

eQTL analysis

Using a curated collection of 6 eQTL datasets in adipose-related tissues, index SNPs at newly identified ectopic fat loci were examined in association with transcript expression. Datasets were collected through publications, publically available sources, or private collaboration. The eQTL datasets met criteria for statistical thresholds for SNP-gene transcript

associations as described in the original papers and were limited to index SNPs and SNPs in LD with the index SNP ($r^2 > 0.8$) across all ancestries available in the 1000 Genomes Project pilot (SNAP³¹). A general overview of the larger collection of more than 50 eQTL studies from which the adipose-related datasets (omental, visceral and subcutaneous adipose,³⁸⁻⁴²) were derived from has been published.⁴³ Additional eQTL data was integrated from online sources including ScanDB, the Broad Institute GTEx Portal, and the Pritchard Lab (eqtl.uchicago.edu). Results for GTEx Analysis V4 for subcutaneous adipose tissue were downloaded from the GTEx Portal and then additionally filtered as described below (www.gtexportal.org⁴¹). Splicing QTL (sQTL) results generated with sQTLseeker with false discovery rate $P \leq 0.05$ were retained. For all gene-level eQTLs, if at least 1 SNP passed the tissue-specific empirical threshold in GTEx, the best SNP for that eQTL was always retained. All gene-level eQTL SNPs with $P < 1.67 \times 10^{-11}$ were also retained, reflecting a global threshold correction of $P = 0.05 / (30,000 \text{ genes} \times 1,000,000 \text{ tests})$.

Cis-eQTL analysis showed SNPs at *ENSA* (a locus identified in association with PAT) was correlated with multiple transcripts (*MRPS21*, *CTSK* and *LASS2*, $P < 10^{-4}$) in subcutaneous and omental adipose tissue (Supplementary Table 16), suggesting these may be the relevant transcripts at this locus and not *ENSA*, the closest gene to the lead association signal. However, the *ENSA* locus was not selected for functional validation, as there were too many genes in the region to practically follow up. No other eQTLs were identified.

Characterization in Model Organisms

Selection of Loci for Characterization

For functional follow-up and characterization of ectopic fat loci, four gene-trait associations were selected based on visual examination of regional association plots (Supplementary Figures 1a-g) for a localized association within a gene body at each locus (*RREB1*, *ATXN1* and *UBE2E2*) or localized association near the gene body and the lack of

other genes within 1Mbp of the lead SNP (*EBF1*) to increase the probability of experimentally testing the likely causal gene in murine models.

Mouse studies

Experiments were approved by and in compliance with the ethical regulations of the Harvard Medical Area Standing Committee on Animals. Male C57BL/6 mice were purchased from Charles River and housed at $22 \pm 2^{\circ}\text{C}$, with a 12h light (0700-1900 h), 12h dark (1900-0700 h) cycle and *ad libitum* access to food and water. With the exception of the data shown in Supplementary Figure 6, experiments were conducted in male mice. Diet-induced obesity was modeled with high fat (D12492) and control chow (D12450J) matched for sucrose content (Research Diets, Inc.). Adipose tissue was harvested, homogenized in Trizol (Life Technologies), and RNA extracted according to the manufacturers protocol. cDNA was synthesized using the High-Capacity cDNA Reverse Transcription Kit (Life Technologies). qPCR was performed using iTaq Universal SYBR Green Supermix (Bio-Rad, Hercules, CA) on an iCycler (Bio-Rad) instrument. See Supplementary Table 17 for primer sequences used in these analyses. Gene expression was normalized to 18S. The delta-delta CT method was utilized to calculate fold change in transcript levels.

*Comparison of baseline adipose-specific expression of *Atxn1**

Given that the SNP-ectopic fat association for *ATXN1* was confined to men, we assessed gender-specific effects in mice of *Atxn1* expression. There was no detectable gender effect on the baseline, adipose-specific expression of *Atxn1* (Supplementary Figure 6).

Adipogenesis assay

Adipose tissue from C57BL/6 mice was minced and digested with collagenase D (Roche) in a shaking water bath (37C, 225rpm, 40min). The digest was centrifuged at 400g for

10 min. Pelleted stromal vascular cells were filtered (40µm) and then washed with PBS and subjected to additional negative selection (CD31⁻ / lineage⁻) adapted from previously performed methods⁴⁴ using antibody coated microbeads (Miltenyi Biotec). Cells were cultured to confluence in collagen-coated plates and stimulated with dexamethasone, insulin and 3-isobutyl-1-methylxanthine to induce adipogenic differentiation. For genetic loss of function assays, validated shRNA sequences (Broad, *Ube2e2*: TRCN0000040962; *Atxn1*: TRCN0000240655) or scramble sequence were subcloned into a retroviral vector (pMKO.1). Gene knock-down efficiency was confirmed by qPCR in 3T3L1 cells, in each instance reproducibly achieving a minimum of 60% reduction of transcriptional activity. Differentiation into mature lipid-containing adipocytes was determined by oil-red-o (ORO) staining and quantified by measuring alcohol-extracted ORO dye at optical density 520 nm (OD₅₂₀).

Cohort Specific Acknowledgements and Funding

Please see the Supplementary Note for acknowledgements and funding statements from all participating cohorts.

772 METHODS REFERENCES

- 773 28. Zillikens, M. C. *et al.* Sex-specific genetic effects influence variation in body composition.
774 *Diabetologia* **51**, 2233-2241, doi:10.1007/s00125-008-1163-0 (2008).
- 775 29. Li, Y., Willer, C. J., Ding, J., Scheet, P. & Abecasis, G. R. MaCH: using sequence and
776 genotype data to estimate haplotypes and unobserved genotypes. *Genet. Epidemiol.* **34**,
777 816-834, doi:10.1002/gepi.20533 (2010).
- 778 30. Howie, B. N., Donnelly, P. & Marchini, J. A flexible and accurate genotype imputation
779 method for the next generation of genome-wide association studies. *PLoS genetics* **5**,
780 e1000529, doi:10.1371/journal.pgen.1000529 (2009).
- 781 31. Johnson, A. D. *et al.* SNAP: a web-based tool for identification and annotation of proxy
782 SNPs using HapMap. *Bioinformatics* **24**, 2938-2939, doi:10.1093/bioinformatics/btn564
783 (2008).
- 784 32. Manning, A. K. *et al.* A genome-wide approach accounting for body mass index identifies
785 genetic variants influencing fasting glycemic traits and insulin resistance. *Nat. Genet.* **44**,
786 659-669, doi:10.1038/ng.2274 (2012).
- 787 33. Global Lipids Genetics, C. *et al.* Discovery and refinement of loci associated with lipid
788 levels. *Nat. Genet.* **45**, 1274-1283, doi:10.1038/ng.2797 (2013).
- 789 34. Coronary Artery Disease Genetics, C. A genome-wide association study in Europeans
790 and South Asians identifies five new loci for coronary artery disease. *Nat. Genet.* **43**,
791 339-344, doi:10.1038/ng.782 (2011).
- 792 35. Schunkert, H. *et al.* Large-scale association analysis identifies 13 new susceptibility loci
793 for coronary artery disease. *Nat. Genet.* **43**, 333-338, doi:10.1038/ng.784 (2011).
- 794 36. International Consortium for Blood Pressure Genome-Wide Association, S. *et al.* Genetic
795 variants in novel pathways influence blood pressure and cardiovascular disease risk.
796 *Nature* **478**, 103-109, doi:10.1038/nature10405 (2011).
- 797 37. Feng, S., Wang, S., Chen, C. C. & Lan, L. GWAPower: a statistical power calculation
798 software for genome-wide association studies with quantitative traits. *BMC Genet.* **12**,
799 12, doi:10.1186/1471-2156-12-12 (2011).
- 800 38. Emilsson, V. *et al.* Genetics of gene expression and its effect on disease. *Nature* **452**,
801 423-428, doi:10.1038/nature06758 (2008).
- 802 39. Greenawalt, D. M. *et al.* A survey of the genetics of stomach, liver, and adipose gene
803 expression from a morbidly obese cohort. *Genome Res.* **21**, 1008-1016,
804 doi:10.1101/gr.112821.110 (2011).
- 805 40. Grundberg, E. *et al.* Mapping cis- and trans-regulatory effects across multiple tissues in
806 twins. *Nat. Genet.* **44**, 1084-1089, doi:10.1038/ng.2394 (2012).
- 807 41. Consortium, G. T. The Genotype-Tissue Expression (GTEx) project. *Nat. Genet.* **45**,
808 580-585, doi:10.1038/ng.2653 (2013).
- 809 42. Foroughi Asl, H. *et al.* Expression quantitative trait Loci acting across multiple tissues
810 are enriched in inherited risk for coronary artery disease. *Circ. Cardiovasc. Genet.* **8**,
811 305-315, doi:10.1161/CIRCGENETICS.114.000640 (2015).
- 812 43. Zhang, X. *et al.* Synthesis of 53 tissue and cell line expression QTL datasets reveals
813 master eQTLs. *BMC Genomics* **15**, 532, doi:10.1186/1471-2164-15-532 (2014).
- 814 44. Kim, S. M. *et al.* Loss of white adipose hyperplastic potential is associated with
815 enhanced susceptibility to insulin resistance. *Cell metabolism* **20**, 1049-1058,
816 doi:10.1016/j.cmet.2014.10.010 (2014).
- 817